# 1

# Introduction

Throughout the last several decades, significant activity has occurred in the development of photonic devices that can confine, control, and route light on a scale commensurate with modern electronic devices, namely the nanometer scale. A key motivation for this activity is the promise of photonic devices, and the corresponding circuits comprised thereof, having a density approaching that of modern electronic circuits. However, for this promise to be realized, such devices must possess the ability to confine light on a subwavelength scale, and they must be fabricated in a material system that is compatible with the microelectronics manufacturing infrastructure. Although the latter requirement is readily satisfied through a proper choice of materials, i.e., silicon, the former was historically more elusive. The reason for this originates from the nature of confinement in conventional materials: Reflective, i.e., conducting, materials are lossy at optical wavelengths, whereas refractive, i.e., dielectric, materials do not confine optical modes on a sufficiently small scale. In the search for a solution, researchers have turned to the field of photonic-crystal (PhC) devices and their associated photonic-bandgap devices, which offer both low loss and high confinement, and they can be readily fabricated in silicon.

To a large extent, the field of PhCs can be thought of as having it origins in the conventional one-dimensional (1D) thin-film stack, wherein layers of two or more different optical materials are arranged in a periodic fashion. In such devices, it is well known that certain frequencies are transmitted while others are not. As the index contrast between the alternating layers is increased, the selectivity of the transmitted and reflected wavelengths is also increased. When generalized to two and three dimensions, this selectivity is what gives rise to high mode confinement.

Although 1D thin-film stacks have been known for over a century, their generalization to higher dimensions was not proposed until the 1970s by Bykov [1–4] as a possible means of inhibiting spontaneous emission. In essence, Bykov proposed the use of a periodic structure that served to inhibit certain electromagnetic frequencies, thereby disallowing spontaneous emission. This type of structure has recently come to be called a "photonic crystal," and it can inhibit the propagation of light over a certain band of wavelengths, while allowing other bands to propagate. Such behavior may give rise to a "photonic bandgap" (PBG), which is analogous to the electronic bandgap

*Photonic Crystals: Theory, Applications, and Fabrication.* By D. W. Prather, S. Shi, A. Sharkawy, J. Murakowski, and G. J. Schneider
Copyright © 2009 John Wiley & Sons, Inc.

COPYRIGHTED MATERIAL

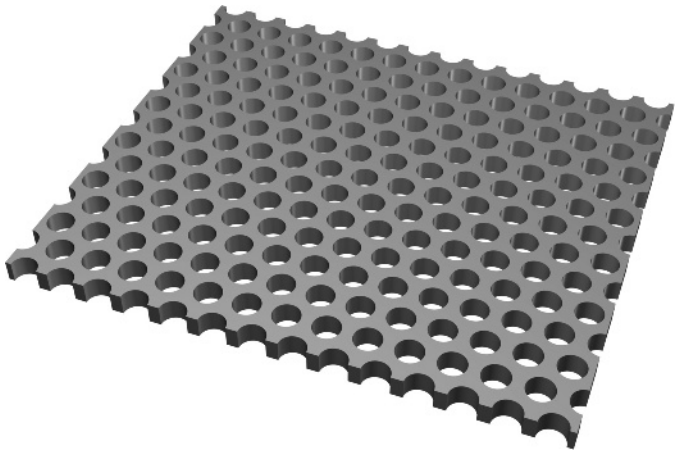

**Figure 1.1** Periodic structure of air holes in a high-index finite-height substrate. Such a structure can prohibit propagation for a certain band of frequencies called a photonic bandgap.

in semiconductor materials (see Section 1.2). An example of a simple, easily fabricated periodic structure that may exhibit the property of a bandgap is shown in Fig. 1.1.

These devices ultimately became known as PBG structures, as they suppress band(s) of frequencies from existing within them, the so-called photonic bandgap(s). In a similar vein, Yablonovitch [5] proposed a structure in which an electronic and photonic gap are overlapped in energy; such a structure would be incapable of light emission by recombination, which thereby makes it possible to enhance the performance of lasers, heterojunctions, bipolar transistors, and solar cells. Subsequent to this work, John [6] proposed using such structures for the localization of light in strongly scattering dielectric structures. In each of these cases, the underlying idea was to tailor the properties of photons (i.e., electromagnetic modes) in a material in a manner analogous to that of electrons in atomic crystals. That is to say, in the electronic case, the wave functions of electrons interact with the periodic potential of the atomic lattice, and for a certain range of energies (analogous to frequencies for photons), electronic states do not exist, thus giving rise to an electronic bandgap. For PhCs, the analog of the electronic potential in an atomic crystal is the periodic variation of the dielectric constants of the various constituent materials of the PhC structure. Likewise, because of the periodic interaction, photonic bandgaps appear, in which certain modes, or frequencies, are forbidden. Futhermore, in such a structure, one can introduce one or more line or point defects, which locally disrupt the periodic lattice, wherein a localized mode may exist with a frequency inside the bandgap; such modes are confined to the region of the defect by virtue of being suppressed within the surrounding lattice. For this reason, these devices offer extreme mode confinement as well as the ability to control and route light compactly and efficiently.

With these advances, the field of PhCs, and in particular their realization in silicon-based materials, has been an active field of research over the last several decades. During this time, great success has been achieved in identifying suitable periodic

structures, dielectric materials, and both theoretical as well as experimental demonstration and characterization of one-, two-, and three-dimensional (3D) PhC and bandgap structures. Therefore, it is the goal of this book to provide an introduction to these advances and to lay the underlying foundation for the design tools and fabrication processes necessary to promote their continued development.

## 1.1 HISTORICAL OVERVIEW

To a large extent, the more recent interest in PhCs can be attributed to the early papers of Yablonovitch [5] and John [6]. Both of these papers were, more or less, theoretical assertions; following their publication, the quest was on to demonstrate an actual bandgap device experimentally. To this end, Yablonovitch and Gmitter [7] fabricated a face-centered-cubic (FCC) lattice on a large scale (microwave frequencies) and measured the transmission spectra at various angles, in the hope of observing a complete photonic bandgap. Unfortunately, they did not find one. For this reason, theorists were motivated to investigate the problem systematically [8–12]. Accordingly, they first attempted to solve Maxwell's equations in 3D using the scalar-wave approximation [13], which predicted gaps for FCC the structure, contrary to experimental results. Subsequent solutions incorporating the vector nature of the electromagnetic field were developed, based on the plane-wave expansion method [9, 10, 14, 15]. Application of these tools showed that the FCC structure did not have a complete bandgap [9, 10]. Subsequently, Soukoulis proposed the use of a diamond lattice to reduce the degeneracy of the FCC lattice, and a complete bandgap was found for spheres with a dielectric constant of 3.6. Yablonovitch et al. then proceeded to fabricate the diamond structure by drilling cylindrical holes into the dielectric material [16]. Transmission measurements for this new structure showed a complete bandgap, in agreement with theory.

After this initial success, the field of photonic bandgap devices grew at an exponential rate. Additional structures were proposed to exhibit bandgaps, such as the so-called "woodpile" structure shown in Fig. 1.2, which also has diamond symmetry. The appealing aspect of this structure was that it could be made in a layer-by-layer manner by stacking alumina rods in a criss-cross fashion. To validate earlier theoretical calculations performed on the structure, different transmission measurements were collected and were found to agree with theoretical results. Furthermore, this device was scaled down by stacking perforated silicon wafers in a square pattern, which extended the frequency of the gap into the terahertz regime [17–20]. To obtain a bandgap in the infrared regime [21], the woodpile structure was fabricated using silicon processing techniques. When further scaling was attempted, down to micrometer and submicrometer regime, alignment between subsequent layers became increasingly more challenging and resulted in a marked reduction in sample yield.

For micron-scale photonic-bandgap structures, some researchers turned to the colloidal self-organization of monodisperese spheres [22], knowing that natural opals exhibit the interesting property wherein color of reflected light changed when viewed at different angles under white-light illumination. Along these lines, optical

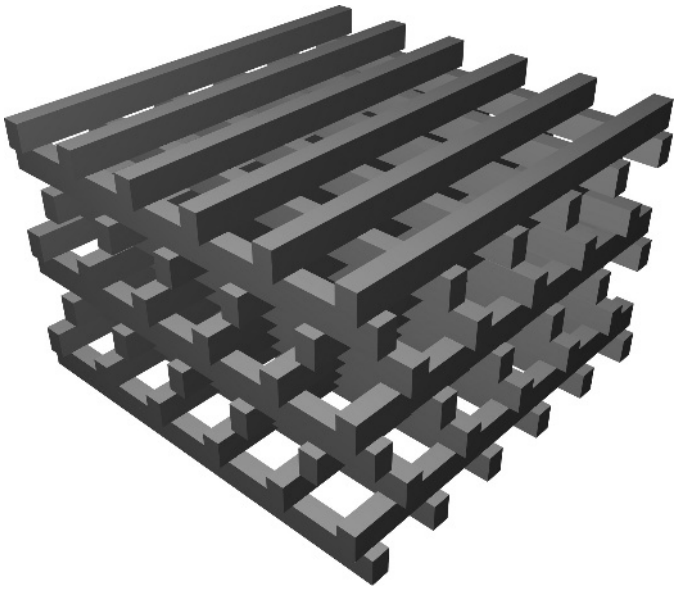

**Figure 1.2** A three-dimensional photonic-crystal structure (woodpile).

properties such as transmission, reflection, diffraction, and dispersion were measured in artificial opal structures made from monodisperse polystyrene colloids [23–32]. Transmission data showed dips that corresponded to directional stop bands on a wavelength scale comparable with the spacing of the spheres.

However, a crucial drawback of full three-dimensional and self-organizing photonic-bandgap structures is that, once fabricated, the bandgap behavior cannot be easily altered or engineered for a particular function or application. In addition, the controlled introduction of defects (doping) is hard to achieve, which in the end has significantly limited their use.

To overcome this limitation, Joannopoulos et al. [33] introduced the planar PhC waveguide to guide optical light in air along narrow channels and around very tight bends with minimal loss [34–39]. This structure uses two-dimensional periodicity that consists of infinitely long silicon pillars in an air background [40]. By introducing a point defect, Villeneuve et al. [41] were able to design a high-$Q$ nanocavity in the same structure, which supported a single localized mode. The cavity was made by introducing a point defect locally into a lattice cell surrounded by a sufficient number of layers to achieve high $Q$ value. Villeneuve et al. also fabricated a one-dimensional optical filter from an air-bridge nanocavity that consisted of a channel waveguide and a one-dimensional PhC suspended in air [42, 43]. Channel-drop filters were later studied by Fan and colleagues [44, 45], who used two waveguides and an optical resonator system of two single-mode cavities, and another structure with a single cavity that supports doubly degenerate hexapole states, to achieve wavelength filtering [46, 47]. Fan et al. [48] later analyzed the effect of waveguide branching in PhCs using two resonant cavities with equal decay rates in the branched waveguides. Povinelli et al. [49] presented a study in which they constructed quasi-two-dimensional (2D) defect modes

in a three-dimensional (3D) PhC structure [49]. Such modes had a striking similarity to those found in 2D PhCs in terms of polarization, field profile, and projected band structures.

Following this work, Johnson studied the effect of finite height on two-dimensional photonic-bandgap structures in terms of bandgap size and confinement in photonic-crystal slabs [50]. He found that, when going from infinite- to finite-height photonic-bandgap structures, the size of the bandgap would shrink about 40% because of radiation losses imposed by the finite height of the structure. Johnson et al. [51] also studied the effect of cross talk in waveguide intersections. He used resonant tunneling to achieve nearly 100% throughput and 0% cross talk between crossing perpendicular PhC waveguides.

It is also important to point out key contributions to materials systems, such as III–V materials. In this area, Scherer and colleagues [52–55] demonstrated photonic-crystal structures in perforated slabs of GaAsP. They used electron-beam lithography followed by a sequence of dry etching steps to define PhC structures with 350-nm spacings in GaAsP and GaAs epilayers. Similar structures were later fabricated also in InGaAsP, which led to the fabrication of a two-dimensional photonic-bandgap defect-mode laser designed for a peak emission wavelength of 1.55 micrometers at room temperature [56–61]. Lee et al. [62, 63] measured the spontaneous emission power spectrum of the fabricated structure. Theoretical studies of the fabricated structures were presented by Vučković and colleagues [64, 65].

Following this work, Yoshie et al. [66] later characterized different modes within two-dimensional PhC nanocavities with self-organized InAs quantum dots as an active material. They observed highly localized donor-mode resonances with 3–5-nm line widths. Additionally, Lončar et al. [67, 68] introduced line defects to PhC slab structures to resemble an optical wire or waveguide. Meanwhile, Adibi et al. [69, 70] explored different techniques to control the positions of guided modes as well as the number of guided modes within a waveguide, eventually leading to the design of single-mode PhC waveguides in a perforated slab of air holes. Photonic-crystal waveguides were also presented using coupled cavities by Bayindir et al. [71–74] and Özbay et al. [75]. They demonstrated theoretically and experimentally that photons can propagate through strongly localized defect cavities because of coupling between adjacent cavity modes based on the tight-binding formalism also used in solid-state physics [76]. They observed a high transmission of electromagnetic waves through the cavities even when they were placed along an arbitrarily shaped path.

Strong directionally dispersive optical properties in PhCs were studied and explored for so-called "superprism" applications by Kosaka et al. [77–79], who demonstrated extraordinary angle sensitivity of light propagation. In this work, a transmitted beam was swung from $-70^\circ$ to $+70^\circ$ with a slight change in the incident angle within $\pm 7^\circ$. This phenomenon implies the presence of a negative effective refractive [80] index, and it was used for applications such as beam steering, spot size conversion, and self-collimation [81].

Two-dimensional photonic crystals can be realized by using either a periodic array of dielectric rods of any shape and/or geometry or a perforated dielectric slab of air holes. Such structures can be further optimized to achieve either a wider or a narrower bandgap based on the desired application. Two-dimensional photonic crystals impose

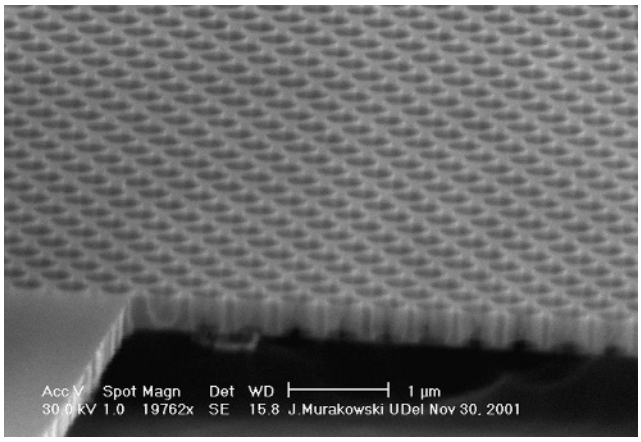


**Figure 1.3** Scanning electron microscopy (SEM) picture of a periodic array of air holes in a suspended Si membrane (slab photonic crystal).

periodicity in two dimensions, whereas the third dimension either is practically infinitely long (photonic-crystal fibers) or has a finite height (photonic-crystal slabs). Three-dimensional photonic crystals impose periodicity in all three dimensions. An example of a three-dimensional photonic crystal is the woodpile structure in Fig. 1.2.

Because they are easier to analyze and fabricate, two-dimensional photonic crystals have attracted the attention of many researchers and engineers. An example of a fabricated two-dimensional photonic crystal is shown in Fig. 1.3. Planar photonic-crystal devices, such as splitters [48, 71, 82–84], high-$Q$ microcavities [35, 41, 56, 58, 85–87], and channel drop/add filters [44, 45, 88, 89], have been investigated both theoretically [50, 69, 90] and experimentally [52, 55, 59, 91–94].

## 1.2 ANALOGY BETWEEN PHOTONIC AND SEMICONDUCTOR CRYSTALS

Understanding the relationship between electronic band structure and photonic band structure requires an examination of the basic equations that govern the motion of electrons and photons, which are called the Schrödinger equation and Maxwell's equations, respectively. When applied to the problems of electrons in crystalline solids and photons in periodic dielectric media, respectively, analogies between the two governing relations become apparent. To make the most of these analogies, it is important to examine both the similarities and the differences.

In a semiconductor crystal, electron behavior is governed by quantum mechanics [95]. The electron is described using the Schrödinger equation

$$\underbrace{\left[\frac{-h^2}{8\pi^2 m^*}\nabla^2 + V(\mathbf{r})\right]}_{\text{Hamiltonian operator}} \varphi(\mathbf{r}) = E\varphi(\mathbf{r}), \tag{1.1}$$

where $h$ is Planck's constant, $m^*$ is the effective mass [76] of the electron, $V(\mathbf{r})$ is the potential function, $\varphi(\mathbf{r})$ is the wave function of the electron, and $E$ is the total energy. The wave function $\varphi(\mathbf{r})$ in quantum physics can be interpreted as a *probability amplitude* function, i.e., the probability of a measurement finding the electron within a volume element $dV$, located at a position denoted by $\mathbf{r}$, is given by $|\varphi(\mathbf{r})|^2 dV$. For a crystal lattice, in the absence of defects, the potential is periodic; i.e., $V(\mathbf{r}) = V(\mathbf{r} + \mathbf{R})$, where $\mathbf{R}$ is a vector that represents the displacement between any two lattice sites. In this case, solutions $\varphi(\mathbf{r})$ take the form of propagating waves called *Bloch waves*: plane waves modulated by an amplitude function with the same periodicity as the crystal lattice (see Chapter 2).

The electromagnetic fields are governed by classic electromagnetic theory [96]. The fields are described using Maxwell's equations: four coupled equations that relate the electric and magnetic fields to one another and to any sources of charge or current present. In the absence of magnetic media, two of these four equations can be combined to yield

$$\underbrace{\left[\nabla \times \frac{1}{\varepsilon(\mathbf{r})} \nabla \times\right]}_{\text{Maxwell operator}} \mathbf{H}(\mathbf{r}) = (\omega/c)^2 \mathbf{H}(\mathbf{r}), \tag{1.2}$$

where $\mathbf{H}(\mathbf{r})$ is the magnetic field, $\omega$ is the angular frequency, $c$ is the speed of light in vacuum, and $\varepsilon(\mathbf{r})$ is the dielectric permittivity. In a photonic crystal, the optical properties of the medium are periodic, i.e., $\varepsilon(\mathbf{r}) = \varepsilon(\mathbf{r} + \mathbf{R})$, and solutions are also Bloch waves.

Equations (1.1) and (1.2) are eigenvalue equations with similar forms. Inspection of the two equations reveals certain analogous features. Each equation describes a wavelike function in space: $\varphi(\mathbf{r})$ and $\mathbf{H}(\mathbf{r})$, respectively. Each wave exists in a medium characterized by a periodic material function: the periodic potential $V$ and the periodic permittivity $\varepsilon$, respectively. These periodic functions each appear within second-order space-differential operators, the Hamiltonian and Maxwell operators, respectively, where both of these operators are Hermitian. The corresponding real eigenvalues are the electron energy $E$ and the squared frequency of the electromagnetic wave $\omega^2$, respectively.

In both the electronic and photonic cases, because of the coherent superposition of the partial scattering of the wave at each lattice site, certain bands exist in the eigenvalue spectrum in which propagation is forbidden, which are called bandgaps. Likewise, in both cases, defects can occur in the periodic medium, which can support trapped or "localized" states with eigenvalues that would be forbidden in the defect-free lattice. As the defect density increases, the probability for the trapped wave to tunnel to a nearby defect site also increases; this permits the propagation of states with eigenvalues inside the bandgap of the bulk crystal. This effect, which is well known in semiconductor applications, is called doping, and it is vital to the usefulness of nearly all semiconductor devices like diodes, transistors, light-emitting diodes (LEDs), and so on. Not surprisingly, defects are also essential to the usefulness of many of the proposed applications of photonic crystals (see Chapter 4).

These analogies between the Schrödinger and Maxwell eigenvalue equations have allowed researchers to apply to PhCs many useful conceptual tools of solid state physics, such as Bloch waves, reciprocal space, Brillouin zones, band structure, conduction and valence bands, and dispersion diagrams. Some of these have already been mentioned briefly in this discussion; a more comprehensive discussion of all these tools can be found in Chapter 2.

Having presented the useful similarities between semiconductor and photonic crystals, completeness demands that we consider the important differences as well. First is the fundamentally different physical nature of the wave: The magnetic field is a vector quantity, whereas the electronic wave function can usually be treated as a scalar (i.e., spin can be ignored). Equation (1.2) contains three scalar equations, one for each component of the vector field. Scalar-wave approximations can yield valuable insights into photonic crystals, but for quantitative comparisons with experiments, a rigorous full vector-wave calculation is required.

Second, no characteristic length scale is inherent in Maxwell's equations. This contrasts with the Schrödinger equation, in which fundamental physical constants, such as Planck's constant and the electron mass, conspire to create fundamental scales of length like the Bohr radius. Scaling the dimensions of a particular electronic problem by a given factor can profoundly change the outcome. The same operation applied to a photonic problem will change only the frequencies of the solution by the scale factor; the solution is otherwise unchanged. This important distinction is of great importance because unlike the atoms that comprise crystalline solids such as semiconductors, the periodically arranged bits of material that constitute the "photonic atoms" of a PhC are generally not naturally occurring and must be designed and fabricated. This process has proved challenging at optical length scales (see Chapter 6). The scale invariance of the Maxwell eigenvalue equation allows proposed structures to be tested at more accessible microwave scales, with confidence that desired properties will be retained if an identical structure is fabricated on a smaller scale (provided that the optical material properties are retained as the frequencies are scaled).

Third, an important distinction exists between the two respective eigenvalues. Because the photonic eigenvalue is proportional to the squared frequency, and $E_{\text{photon}} = h\omega/2\pi$, there are no negative-energy photonic solutions; i.e., no truly bound states are allowed. Nevertheless, it is possible to realize microcavities in PhCs with very high $Q$ values, with correspondingly long lifetimes of confined optical modes.

Finally, in the limit of linear response, the solutions of the photonic eigenvalue problem are uncoupled. In other words, electromagnetic waves obey the principle of superposition and do not interact. (Exceptions to this principle fall in the realm of nonlinear optics.) This behavior is in contrast to the often strong interactions between electrons. For this reason, it has been noted by Yablonovitch [97] that band theory, which assumes that the wave functions of multiple particles are uncorrelated, actually makes more sense for photons than for electrons.

## 1.3 ANALYZING PHOTONIC-BANDGAP STRUCTURES

Only a precious few geometries can be analyzed using exact analytical methods. For most photonic crystals with practical importance, numerical simulations are required

to gain insight into the behavior of light that interacts with them. One method often employed in this case is the plane-wave expansion method (PWEM, described in detail in Chapter 3), which makes use of the fact that normal modes in periodic structures can be expressed as a superposition of a set of plane waves. This way, Eq. (1.2) is converted to a *matrix* eigenvalue problem, which is solved using standard numerical techniques to obtain the dispersion relations inside a photonic crystal [9, 10, 15, 98]. The solutions are eigenfrequencies, which are plotted as a function of wave vectors tracing the edges of an irreducible Brillouin zone, to form a dispersion diagram; examples are shown in Fig. 1.4. The dispersion diagram is a graphical representation of the frequencies that correspond to waves propagating within a photonic-crystal lattice with various wave vectors. Although a two-dimensional dispersion diagram (depicting only those wave vectors on the irreducible Brillouin-zone edge) is sufficient to determine whether a bandgap exists for a certain photonic crystal, it is not sufficient to indicate the presence of other interesting and useful dispersive behaviors, such as negative refractive-index phenomena or the superprism effect (see Chapter 5). In these cases, a three-dimensional plot of the dispersion surface, depicting eigenfrequencies as a function of all wave vectors within the full Brillouin zone, provides a more detailed view of a photonic crystal's supported modes at frequencies both inside and outside any bandgap. An example of such a diagram is shown in Fig. 1.5, where a dispersion surface that represents just one of the higher bands is displayed.

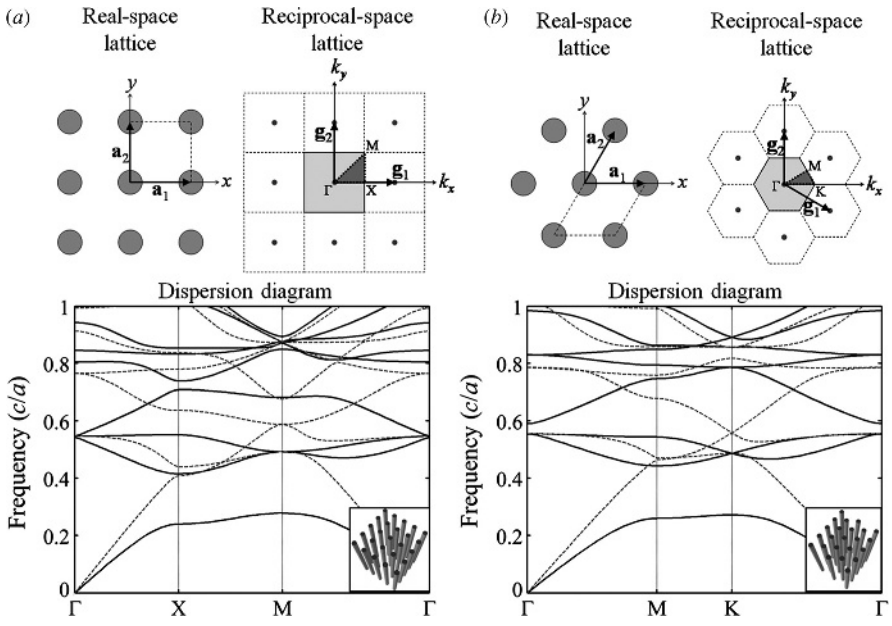


**Figure 1.4** PWEM used to analyze different two-dimensional PhC structures with (a) square or (b) triangular lattices. Eigenfrequencies are determined for Bloch wave vectors around the edge of an irreducible Brillouin zone, which is indicated by a dark shaded triangle for each lattice. The result is a dispersion diagram showing the allowed frequencies for different wave vectors within the lattice. The two separable polarization modes, known as transverse electric (TE) and transverse magnetic (TM), are indicated by dashed and solid curves, respectively.

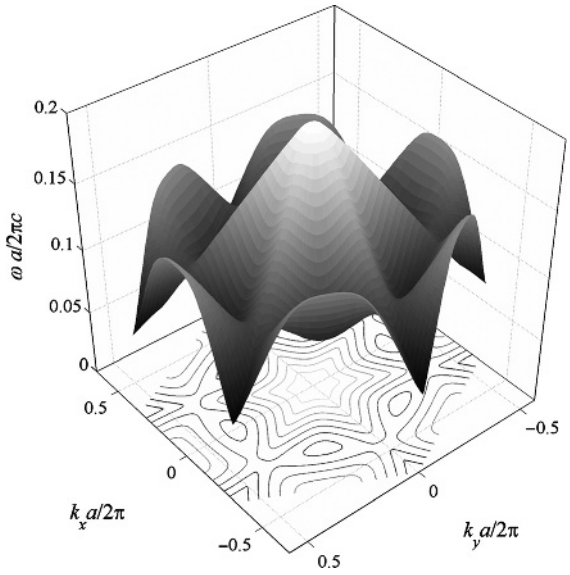


**Figure 1.5** Dispersion surface. The horizontal plane spans both Bloch wave vector components $k_x$ and $k_y$. The vertical axis gives the normalized frequency $\omega a/2\pi c = a/\lambda$.

Although the PWEM allows for analyzing the dispersion properties of a PhC structure, it is still limited because transmission spectra, field distributions, and backreflections from finite-size structures cannot be directly determined. Therefore, an alternative approach has been adopted, which is based on a numerical solution of Maxwell's equations in real space using the finite-difference time-domain (FDTD) method (also described in detail in Chapter 3). The FDTD method has been used to

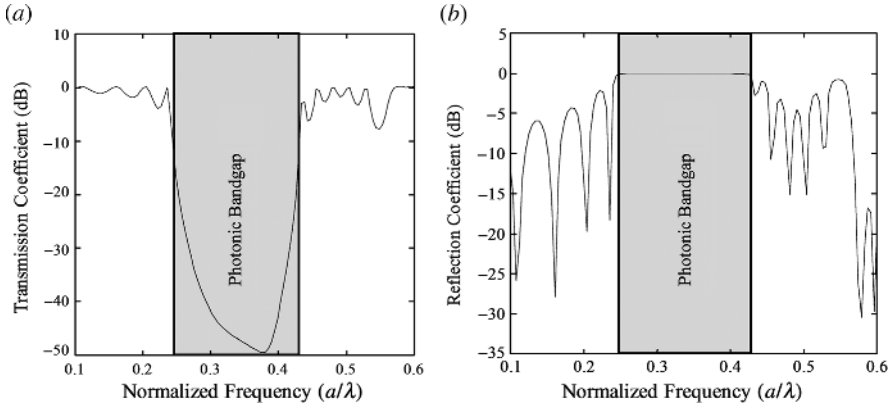


**Figure 1.6** Transmission (a) and reflection (b) for six layers of a 2D photonic-crystal structure composed of a square lattice of silicon ($\varepsilon_r = 11.56$) rods in air ($\varepsilon_r = 1$), with $r/a = 0.2$, obtained using FDTD. Low transmission and near-perfect reflectivity is observed within the bandgap.

analyze multichannel drop/add filters [88] and calculate the transmission through sharp waveguide bends [36], as well as in the study of a waveguiding mechanism through localized coupled cavities in three-dimensional photonic crystals [72, 99].

To illustrate the use of FDTD on finite-size PhC structures, consider a 2D PhC structure consisting of a square lattice of silicon rods in air background. The transmission coefficient as a function of frequency for six layers of such a photonic crystal is shown in Fig. 1.6a, and the reflection coefficient is shown in Fig. 1.6b. The photonic bandgap can be observed in these figures as a frequency range of low transmission and high reflectivity, because the electromagnetic wave penetrates into the PhC only to a limited depth before being attenuated by the destructive interference of the forward-scattered waves that emerge from the periodic lattice of scattering objects. The bandgap has a center frequency at $a/\lambda_{\text{center}} = 0.339$ and a bandgap size $\Delta f/f_{\text{center}}$ equal to 55.4%. This structure can in principle operate for any range of frequencies, from microwave to optical; all results are expressed in units normalized to the operating wavelength. For example, consider the near-infrared frequency regime widely used in telecommunications. If we wish to operate at $\lambda_{\text{center}} = 1550$ nm, then the structure will have a lattice constant equal to $a = 525.5$ nm, and the silicon rods will have a radius of $r = 105$ nm.

In the remainder of this book, following a brief introduction to the interaction of electromagnetic field with periodic dielectric structures in Chapter 2, the numerical methods employed in analyzing them are presented in Chapter 3. Chapters 4 and 5 discuss the applications of photonic crystals taking advantage of the photonic bandgap and of the unique dispersive properties, respectively. A variety of methods developed for the fabrication of 2D and 3D photonic crystals are described in Chapter 6.

## REFERENCES

1. V. Bykov, "Spontaneous Emission in a Periodic Structure," *Zhurnal Experimentalnoi i Teoreticheskoi Fiziki*, vol. 62, 1972.
2. V. Bykov, "Sponteneous Emission in a Periodic Structure," *Soviet Physics JETP*, vol. 35, pp. 269–273, 1972.
3. V. Bykov, "Spontaneous Emission from a Medium with a Band Spectrum," *Sov. J. Quant. Electron.*, vol. 4, pp. 861–871, 1975.
4. V. Bykov, "Free Oscillations of Elastic Dipole Located in Periodic Structure," *Zhurnal Tekhnicheskoi Fiziki*, vol. 48, 1978.
5. E. Yablonovitch, "Inhibited Spontaneous Emission in Solid-State Physics and Electronics," *Phys. Rev. Lett.*, vol. 58, pp. 2059–2062, 1987.
6. S. John, "Strong Localization of Photons in Certain Disordered Dielectric Superlattices," *Phys. Rev. Lett.*, vol. 58, pp. 2486–2489, 1987.
7. E. Yablonovitch and T. J. Gmitter, "Photonic Band Structure: The Face-Cenetered-Cubic Case," *Phys. Rev. Lett.*, vol. 63, pp. 1950–1953, 1989.
8. J. D. Joannopoulos, P. R. Villeneuve, and S. H. Fan, "Photonic Crystals," *Sol. Stat. Comm.*, vol. 102, pp. 165–173, 1997.

9. Z. Zhang and S. Satpathy, "Electromagnetic Wave Propagation in Periodic Structures: Bloch Wave Solution of Maxwell's Equations," *Phys. Rev. Lett.*, vol. 65, pp. 2650–2653, 1990.
10. K. M. Leung and Y. F. Liu, "Photon Band Structures: The Plane-Wave Method," *Phys. Rev. B*, vol. 41, pp. 10188–10190, 1990.
11. S. John and R. Rangarajan, "Optimal Structures for Classical Wave Localization—an Alternative to the Ioffe-Regel Criterion," *Phys. Rev. B*, vol. 38, pp. 10101–10104, 1988.
12. E. N. Economou and A. Zdetsis "Classical Wave Propagation in Periodic Structures," *Phys. Rev. B*, vol. 40, pp. 1334–1337, 1989.
13. S. Datta, C. Chan, K. Ho, and C. M. Soukoulis, "Photonic Bandgaps in Periodic Dielectric Structures—The Scalar Wave Approximation," *Phys. Rev. B*, vol. 46, pp. 10650–10656, 1992.
14. M. Plihal and A. A. Maradudin, "Photonic Band Structure of Two-Dimensional Systems: The Triangular Lattice," *Phys. Rev. B*, vol. 44, pp. 8565–8571, 1991.
15. L. Liu and J. T. Liu, "Photonic Band Structure in the Nearly Plane Wave Approximation," *Eur. Phys. J. B*, vol. 9, pp. 381–388, 1999.
16. E. Yablonovitch, T. J. Gmitter, and K. M. Leung, "Photonic Band-Structure—the Face-Centered-Cubic Case Employing Nonspherical Atoms," *Phys. Rev. Lett.*, vol. 67, pp. 2295–2298, 1991.
17. E. Özbay, A. Abeyta, G. Tuttle, M. C. Tringides, R. Biswas, M. M. Sigalas, and C. M. Soukoulis, "Measuerment of a Three-Dimensional Photonic Band Gap in a Crystal Structure Made of Dielectric Rods," *Phys. Rev. B*, vol. 50, pp. 1945–1948, 1994.
18. E. Özbay, E. Michel, G. Tuttle, R. Biswas, M. M. Sigalas, and K. M. Ho, "Micromachined Millimeter-Wave Photonic Band-Gap Crystals," *Appl. Phys. Lett.*, vol. 64, pp. 2059–2061, 1994.
19. E. Özbay, E. Michel, G. Tuttle, R. Biswas, K. M. Ho, J. Bostak, and M. Bloon, "Double-Etch Geometry for Millimeter-Wave Photonic Band-Gap Crystals," *Appl. Phys. Lett.*, vol. 65, pp. 1617–1619, 1994.
20. E. Özbay, E. Michel, G. Tuttle, R. Biswas, K. M. Ho, J. Bostak, and M. Bloom, "Terahertz Spectroscopy of Three-Dimensional Photonic Band-Gap Crystal," *Opt. Lett.*, vol. 19, pp. 1155, 1994.
21. S.-Y. Lin and J. G. Fleming, "A Three-Dimensional Optical Photonic Crystal," *J. Lightwave Technol.*, vol. 17, pp. 1944–1947, 1999.
22. S. John and K. Busch, "Photonic Band Gap Formation in Certain Self-Organizing Systems," *Phys. Rev. E*, vol. 58, pp. 3896–3908, 1998.
23. İ. İ. Tarhan and G. Watson, "Analytical Expression for the Optimized Stop Bands of Fcc Photonic Crystals in the Scalar-Wave Approximation," *Phys. Rev. B*, vol. 54, pp. 7593–7597, 1996.
24. İ. İ. Tarhan, M. P. Zinkin, and G. Watson, "An Interferometric Technique for Measurement of Photonic Band Structure in Colloidal Crystals," *Opt. Lett.*, vol. 20, pp. 1571–1574, 1995.
25. İ. İ. Tarhan and G. Watson, "Photonic Band Structure of Fcc Colloidal Crystals," *Phys. Rev. Lett.*, vol. 76, pp. 315–318, 1996.
26. İ. İ. Tarhan and G. Watson, "Optical Measurements of Photonic Band Structure in Fcc Colloidal Crystals," C. M. Soukoulis, Ed. in: *Photonic Band Gap Materials*, Norwell, MA, Kluwer Academic, 1996, pp. 93–106.

27. R. D. Pradhan, İ. İ. Tarhan, and G. Watson, "Impurity Modes in the Optical Stop Bands of Doped Colloidal Crystals," *Phys. Rev. B*, vol. 54, pp. 13721–13724, 1996.

28. R. D. Pradhan, J. A. Bloodgood, and G. Watson, "Photonic Band Structure of BCC Colloidal Crystals," *Phys. Rev. B*, vol. 55, pp. 9503–9506, 1997.

29. B. T. Rosner, G. J. Schneider, and G. Watson, "Interferometric Investigation of Photonic Band Structure Effects in Pure and Doped Colloidal Crystals," *J. Opt. Soc. Am. B*, vol. 15, pp. 2654–2658, 1998.

30. Y. Xia, B. Gates, and S. H. Park, "Fabrication of Three-Dimensional Photonic Crystals for Use in the Spectral Region from Ultraviolet to Near-Infrared," *J. Lightwave Technol.*, vol. 17, pp. 1956–1962, 1999.

31. P. Jiang, G. N. Ostojic, R. Narat, D. M. Mittleman, and V. L. Colvin, "The Fabrication and Bandgap Engineering of Photonic Multilayers," *Adv. Mater.*, vol. 13, pp. 389–393, 2001.

32. Y. Xia, B. Gates, and Z.-Y. Li, "Self-Assembly Approaches to Three-Dimensional Photonic Crystals," *Adv. Mater.*, vol. 13, pp. 409–413, 2001.

33. J. D. Joannopoulos, P. R. Villeneuve, and S. Fan, "Photonic Crystals: Putting a New Twist on Light," *Nature*, vol. 386, pp. 143, 1997.

34. E. Chow, S. Y. Lin, J. R. Wendt, S. G. Johnson, and J. D. Joannopoulos, "Quantitative Analysis of Bending Efficiency in Photonic-Crystal Waveguide Bends at 1.55 μm Wavelengths," *Opt. Lett.*, vol. 26, pp. 286–288, 2001.

35. R. D. Meade, A. Devenyi, J. D. Joannopoulos, O. L. Alerhand, D. A. Smith, and K. Kash, "Novel Applications of Photonic Band Gap Materials: Low-Loss Bends and High Q Cavities," *J. Appl. Phys.*, vol. 75, pp. 4753–4755, 1994.

36. A. Mekis, J. C. Chen, I. Kurland, S. Fan, P. R. Villeneuve, and J. D. Joannopoulos, "High Transmission Through Sharp Bends in Photonic Crystal Waveguides," *Phys. Rev. Lett.*, vol. 77, pp. 3787–3790, 1996.

37. S. Fan, J. N. Winn, A. Devenyi, J. C. Chen, R. D. Meade, and J. D. Joannopoulos, "Guided and Defect Modes in Periodic Dielectric Waveguides," *J. Opt. Soc. Am. B*, vol. 12, p. 1267, 1995.

38. A. Mekis, J. Fan, and J. D. Joannopoulos, "Bound States in Photonic Crystal Waveguides and Waveguide Bends," *Phys. Rev. B*, vol. 58, pp. 4809–4917, 1998.

39. S. Y. Lin, E. Chow, V. Hietch, P. R. Villeneuve, and J. D. Joannopoulos, "Experimental Demonstration of Guiding and Bending of Light in a Photonic Crystal," *Science*, vol. 282, p. 274, 1998.

40. J. N. Winn, R. D. Meade, and J. D. Joannopoulos, "Two-Dimensional Photonic Band-Gap Materials," *J. Mod. Opt.*, vol. 41, pp. 257–273, 1994.

41. P. R. Villeneuve, S. Fan, and J. D. Joannopoulos, "Microcavities in Photonic Crystals: Mode Symmetry, Tunability, and Coupling Efficiency," *Phys. Rev. B*, vol. 54, pp. 7837–7842, 1996.

42. P. R. Villeneuve, S. Fan, and J. D. Joannopoulos, "Air-Bridge Microcavities," *Appl. Phys. Lett.*, vol. 67, pp. 167–169, 1995.

43. J. C. Chen, H. A. Haus, J. Fan, P. R. Villeneuve, and J. D. Joannopoulos, "Optical Filters from Photonic Band Gap Air Bridges," *J. Lightwave Technol.*, vol. 14, p. 2575, 1996.

44. H. A. Haus, S. Fan, P. R. Villeneuve, and J. D. Joannopoulos, "Channel Drop Filters in Photonic Crystals," *Opt. Express*, vol. 3, pp. 4–11, 1998.

45. R. Fan, R. Villeneuve, J. D. Joannopoulos, and H. A. Haus, "Channel Drop Tunneling Through Localized States," *Phys. Rev. Lett.*, vol. 80, pp. 960–963, 1998.

46. E. Centeno, B. Guizal, and D. Felbacq, "Multiplexing and Demultiplexing with Photonic Crystals," *J. Opt. A*, vol. 1, pp. L10–L13, 1999.

47. C. Zhang, F. Qiao, J. Wan, and J. Zi, "Enlargement of Nontransmission Frequency Range in Photonic Crystals by Using Multiple Heterostructures," *J. Appl. Phys.*, vol. 87, pp. 3174–3176, 2000.

48. S. Fan, S. G. Johnson, and J. D. Joannopoulos, "Waveguide Branches in Photonic Crystals," *J. Opt. Soc. Am. B*, vol. 18, pp. 162–165, 2001.

49. M. L. Povinelli, S. G. Johnson, J. Fan, and J. D. Joannopoulos, "Emulation of Two-Dimensional Photonic Crystal Defect Modes in a Photonic Crystal with a Three-Dimensional Photonic Band Gap," *Phys. Rev. B*, vol. 64, pp. 753131–753138, 2001.

50. S. G. Johnson, S. Fan, P. R. Villeneuve, and J. D. Joannopoulos, "Guided Modes in Photonic Crystal Slabs," *Phys. Rev. B*, vol. 60, pp. 5751–5758, 1999.

51. S. G. Johnson, C. Manolatou, S. H. Fan, P. R. Villeneuve, J. D. Joannopoulos, and H. A. Haus, "Elimination of Cross Talk in Waveguide Intersections," *Opt. Lett.*, vol. 23, pp. 1855–1857, 1998.

52. C. C. Cheng and A. Scherer, "Fabrication of Photonic Band-Gap Crystals," *J. Vac. Sci. Technol B.*, vol. 13, pp. 2696–2700, 1995.

53. C. C. Cheng, A. Scherer, V. Arbet-Engels, and E. Yablonovitch, "Lithographic Band Gap Tuning in Photonic Band Gap Crystals," *J. Vac. Sci. Technol. B*, vol. 14, pp. 4110–4114, 1996.

54. J. O'Brien, O. Painter, R. Lee, C. C. Cheng, A. Yariv, and A. Scherer, "Lasers Incorporating 2D Photonic Bandgap Mirrors," *Electron. Lett.*, vol. 32, pp. 2243–2244, 1996.

55. C. C. Cheng, A. Scherer, R.-C. Tyan, Y. Fainman, G. Witzgall, and E. Yablonovitch, "New Fabrication Techniques for High Quality Photonic Crystals," *J. Vac. Sci. Technol. B*, vol. 15, pp. 2764–2767, 1997.

56. B. D'Urso, O. Painter, J. O'Brien, T. Tombrello, A. Yariv, and A. Scherer, "Modal Reflectivity in Finite-Depth Two-Dimensional Photonic-Crystal Microcavities," *J. Opt. Soc. Am. B*, vol. 15, pp. 1155–1159, 1998.

57. T. F. Krauss, O. Painter, A. Scherer, J. S. Roberts, and R. M. De La Rue, "Photonic Microstructures as Laser Mirrors," *Opt. Eng.*, vol. 37, pp. 1143–1148, 1998.

58. A. Scherer, O. Painter, B. D'Urso, R. Lee, and A. Yariv, "InGaAsP Photonic Band Gap Crystal Membrane Microresonators," *J. Vac. Sci. Tech. B*, vol. 16, pp. 3906–3910, 1998.

59. O. Painter, J. Vučković, and A. Scherer, "Defect Modes of a Two-Dimensional Photonic Crystal in an Optically Thick Dielectric Slab," *J. Opt. Soc. Am. B*, vol. 16, pp. 275–285, 1999.

60. O. Painter, A. Husain, A. Scherer, J. O'Brien, I. Kim, and P. D. Dapkus, "Room Temperature Photonic Crystal Defect Lasers at Near-Infrared Wavelengths in InGaAsP," *J. Lightwave Technol.*, vol. 17, pp. 2082–2088, 1999.

61. O. Painter, R. K. Lee, A. Scherer, A. Yariv, J. O'Brien, P. D. Dapkus, and I. Kim, "Two-Dimensional Photonic Band-Gap Defect Mode Laser," *Science*, vol. 284, pp. 1819–1821, 1999.

62. R. K. Lee, O. J. Painter, B. Kitzke, A. Scherer, and A. Yariv, "Photonic Bandgap Disk Laser," *Electron. Lett.*, vol. 35, pp. 569–570, 1999.

63. R. K. Lee, O. J. Painter, B. D'Urso, A. Scherer, and A. Yariv, "Measurement of Spontaneous Emission from a Two-Dimensional Photonic Band Gap Defined Microcavity at Near-Infrared Wavelengths," *Appl. Phys. Lett.*, vol. 74, pp. 1522–1524, 1999.
64. Y. Xu, J. Vučković, R. K. Lee, O. J. Painter, A. Scherer, and A. Yariv, "Finite-Difference Time-Domain Calculation of Spotaneous Emission Lifetime in a Microcavity," *J. Opt. Soc. Am. B*, vol. 16, pp. 465–474, 1999.
65. J. Vučković, O. Painter, Y. Xu, A. Yariv, and A. Scherer, "Finite-Difference Time-Domain Calculation of the Spontaneous Emission Coupling Factor in Optical Microcavities," *IEEE J. Quantum Electron.*, vol. 35, pp. 1168–1175, 1999.
66. T. Yoshie, A. Scherer, H. Chen, D. Huffaker, and D. Deppe, "Optical Characterization of Two-Dimensional Photonic Crystal Cavities with Indium Arsenide Quantum Dot Emitters," *Appl. Phys. Lett.*, vol. 79, pp. 114–116, 2001.
67. M. Lončar, D. Nedeljkovic, T. Doll, J. Vučković, A. Scherer, and T. P. Pearsall, "Waveguiding in Planar Photonic Crystals," *Appl. Phys. Lett.*, vol. 77, pp. 1937–1939, 2000.
68. M. Lončar, T. Doll, J. Vučković, and A. Scherer, "Design and Fabrication of Silicon Photonic Crystal Optical Waveguides," *J. Lightwave Technol.*, vol. 18, pp. 1402–1411, 2000.
69. A. Adibi, Y. Xu, R. K. Lee, A. Yariv, and A. Scherer, "Properties of the Slab Modes in Photonic Crystal Optical Waveguides," *J. Lightwave Technol.*, vol. 18, pp. 1554–1564, 2000.
70. A. Adibi, R. K. Lee, Y. Xu, A. Yariv, and A. Scherer, "Design of Photonic Crystal Optical Waveguides with Single Mode Propagation in the Photonic Bandgap," *Electron. Lett.*, vol. 36, pp. 1376–1378, 2000.
71. M. Bayindir, B. Temelkuran, and E. Özbay, "Photonic Crystal Based Beam Splitters," *Appl. Phys. Lett.*, vol. 77, pp. 3902–3904, 2000.
72. M. Bayindir, B. Temelkuran, and E. Özbay, "Propagation of Photons by Hopping: A Waveguiding Mechanism Through Localized Coupled Cavities in Three-Dimensional Photonic Crystals," *Phys. Rev. B*, vol. 61, pp. R11855–R11858, 2000.
73. M. Bayindir, B. Temelkuran, and E. Özbay, "Tight-Binding Description of the Coupled Defect Modes in Three-Dimensional Photonic Crystals," *Phys. Rev. Lett.*, vol. 84, pp. 2140–2143, 2000.
74. M. Bayindir and E. Özbay, "Heavy Photons at Coupled-Cavity Waveguide Band Edges in a Three-Dimensional Photonic Crystal," *Phys. Rev. B*, vol. 62, pp. R2247–R2250, 2000.
75. E. Özbay, M. Bayindir, I. Bulu, and E. Cubukcu, "Investigation of Localized Coupled-Cavity Modes in Two-Dimensional Photonic Bandgap Structures," *IEEE J. Quantum Electron.*, vol. 38, pp. 837–843, 2002.
76. N. W. Ashcroft and N. D. Mermin, *Solid State Physics*, Philadelphia: Saunders College, 1976.
77. H. Kosaka, T. Kawashima, A. Tomita, M. Notomi, T. Tamamura, T. Sato, and S. Kawakami, "Superprism Phenomena in Photonic Crystals," *Phys. Rev. B*, vol. 58, pp. R10096–R10099, 1998.
78. H. Kosaka, T. Kawashima, A. Tomita, M. Notomi, T. Tamamura, T. Sato, and S. Kawakami, "Photonic Crystals for Micro Lightwave Circuits Using Wavelength-Dependent Angular Beam Steering," *Appl. Phys. Lett.*, vol. 74, pp. 1370–1372, 1999.
79. H. Kosaka, T. Kawashima, A. Tomita, M. Notomi, T. Tamamura, T. Sato, and S. Kawakami, "Superprism Phenomena in Photonic Crystals: Toward Microscale Lightwave Circuits," *J. Lightwave Technol.*, vol. 17, pp. 2032–2034, 1999.

80. R. A. Shelby, D. R. Smith, and S. Schultz, "Experimental Verification of a Negative Index of Refraction," *Science*, vol. 292, pp. 77–79, 2001.
81. H. Kosaka, T. Kawashima, A. Tomita, M. Notomi, T. Tamamura, T. Sato, and S. Kawakami, "Self-Collimating Phenomena in Photonic Crystals," *Appl. Phys. Lett.*, vol. 74, pp. 1212–1214, 1999.
82. G. Parker and M. Charlton, "Photonic Crystals," *Physics World*, vol. 13, pp. 29–34, 2000.
83. T. Sondergaard and K. H. Dridi, "Energy Flow in Photonic Crystal Waveguides," *Phys. Rev. B*, vol. 61, pp. 15688–15696, 2000.
84. R. W. Ziolkowski, "FDTD Analysis of PBG Waveguides, Power Splitters and Switches," *Opt. Quantum Electron.*, vol. 31, pp. 843–855, 1999.
85. G. Rarity and C. Weisbuch, Eds. *Microcavities and Photonic Bandgaps: Physics and Applications*. Elounda, Crete: Kluwer Academic Publishers, 1995.
86. H.-B. Sun, V. Mizeikis, Y. Xu, S. Juodkazis, J.-Y. Ye, S. Matsuo, and H. Misawa, "Microcavities in Polymeric Photonic Crystals," *Appl. Phys. Lett.*, vol. 79, pp. 1–3, 2001.
87. S. G. Johnson, F. Shanhui, A. Mekis, and J. D. Joannopoulos, "Multipole-Cancelation Mechanism for High-Q Cavities in the Absence of a Complete Photonic Band Gap," *Appl. Phys. Lett.*, vol. 78, pp. 3388–3390, 2001.
88. A. Sharkawy, S. Shi, and D. W. Prather, "Multichannel Wavelength Division Multiplexing Using Photonic Crystals," *Appl. Opt.*, vol. 40, pp. 2247–2252, 2001.
89. R. Stoffer, H. J. W. M. Hoekstra, R. M. D. Ridder, E. V. Groesen, and F. P. H. V. Beckum, "Numerical Studies of 2D Photonic Crystals: Waveguides, Coupling Between Waveguides and Filters," *Opt. Quantum Electron.*, vol. 32, pp. 947–961, 2000.
90. S. G. Johnson, P. R. Villeneuve, S. Fan, and J. D. Joannopoulos, "Linear Waveguides in Photonic-Crystal Slabs," *Phys. Rev. B*, vol. 62, pp. 8212–8222, 2000.
91. M. Charlton, M. E. Zoorob, G. Parker, M. C. Netti, J. J. Baumberg, J. A. Cox, and H. Kemhadjian, "Experimental Investigation of Photonic Crystal Waveguide Devices and Line-Defect Waveguide Bends," *Mater. Sci. Eng.*, vol. B74, pp. 17–24, 2000.
92. M. Gander, R. McBride, J. Jones, D. Mogilevtsev, T. Birks, J. Knight, and P. Russell, "Experimental Measurement of Group Velocity Dispersion in Photonic Crystal Fibre," *Electron. Lett.*, vol. 35, pp. 63–64, 1999.
93. C. J. M. Smith, R. M. D. L. Rue, M. Rattier, S. Olivier, H. Benisty, C. Weisbuch, P. R. Krauss, R. Houdre, and U. Oesterle, "Coupled Guide and Cavity in a Two-Dimensional Photonic Crystal," *Appl. Phys. Lett.*, vol. 78, pp. 1487–1489, 2001.
94. H. Hirayama, T. Hamano, and Y. Aoyagi, "Novel Surface Emitting Laser Diode Using Photonic Band-Gap Crystal Cavity," *Appl. Phys. Lett.*, vol. 69, pp. 791–793, 1996.
95. R. L. Liboff, Introductory Quantum Mechanics, 4th ed. San Francisco: Addison Wesley, 2003.
96. J. D. Jackson, Classical Electrodynamics, 3rd ed. New York: Wiley, 1999.
97. E. Yablonovitch, "Photonic Band-Gap Structures," *J. Opt. Soc. Am. B*, vol. 10, pp. 283–295, 1993.
98. K. M. Ho, C. T. Chan, and C. M. Soukoulis, "Existence of a Photonic Gap in Periodic Dielectric Structures," *Phys. Rev. Lett.*, vol. 65, pp. 3152–3155, 1990.
99. A. R. McGurn, "Photonic Crystal Circuits: A Theory for Two- and Three Dimensional Networks," *Phys. Rev. B*, vol. 61, pp. 13235–13249, 2000.